Dalton Transactions

RSC Publishing

PAPER

View Article Online
View Journal | View Issue



Cite this: *Dalton Trans.*, 2013, **42**, 935

# Synthesis and X-ray structures of cyclometalated iridium complexes including the hydrides†‡

Chao Wang,[a,b] Hsin-Yi Tiffany Chen,[c] John Bacsa,[b] C. Richard A. Catlow[c] and Jianliang Xiao*[b]

Received 26th June 2012,
Accepted 20th September 2012

DOI: 10.1039/c2dt31368e

www.rsc.org/dalton

Cyclometalation of $[Cp^*IrCl_2]_2$ with ketimine ligands generated very active catalysts for transfer hydrogenation of imines as well as reductive amination. The synthesis and X-ray diffraction structures of three such complexes are disclosed in this paper. The hydrides of two complexes, key intermediates in hydrogenation, have been isolated and their structures determined by X-ray diffraction as well.

## Introduction

The study of cyclometalation has a long history and serves for the development and understanding of C–H activation.[1] The cyclometalation of $[Cp^*IrCl_2]_2$ with aldimine ligands was first studied in detail by Davies and co-workers[2] in 2003 and recently by Jones and co-workers.[3] Applications of cyclometalated Cp*Ir complexes in catalysis only appeared in recent years, however. Successful examples include transfer hydrogenation of ketones,[4] racemerisation of amines,[5] oxidation of water[6] and hydroamination of olefins[7] (Fig. 1). In our study of transfer hydrogenation of imines, we serendipitously discovered that cyclometalated Cp*Ir complexes bearing ketimine ligands are excellent catalysts for imine reduction and reductive amination (Fig. 1).[8,9] In this paper, we disclose the synthesis and X-ray structures of these complexes as well as the first isolation of cyclometalated iridium hydrides, which are key intermediate in transfer hydrogenation of imines and reductive amination.

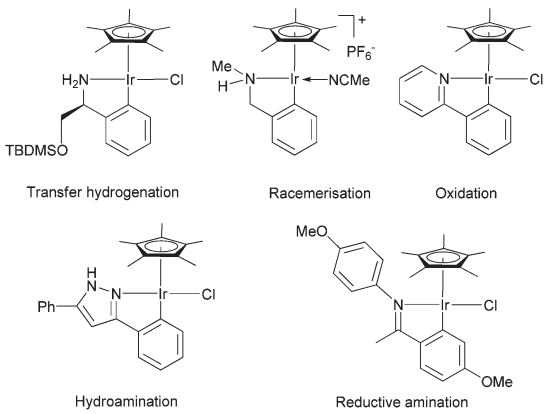


**Fig. 1** Successful cyclometalated metal catalysts.

## Results and discussion

### Synthesis of Cp*Ir–Cl and Cp*Ir–H complexes

Cyclometalation of $[Cp^*IrCl_2]_2$ with aldimines was studied in detail by Davies and co-workers[2] and Jones and co-workers.[3]

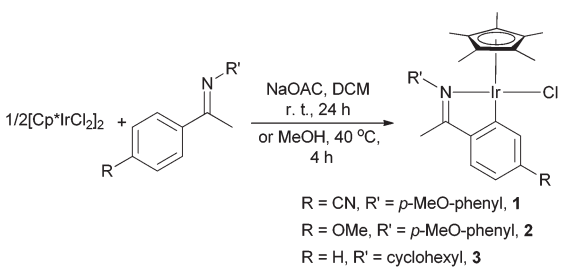


**Scheme 1** Synthesis of cyclometalated iridium chloride complexes.

Although no ketimines were tested in their studies, it turned out that ketimines reacted equally well as aldimines. Thus, the reaction of 1 equivalent of $[Cp^*IrCl_2]_2$ with 2.2 equivalents of ketimine in the presence of 10 equivalents of NaOAc in DCM for 24 h afforded the cyclometalated Cp*Ir complex in good yield (Scheme 1). It was proposed that NaOAc plays an important role in the C–H activation process.[3,10] Interestingly, without any base additive, the reaction proceeded well in

[a]*Key Laboratory of Applied Surface and Colloid Chemistry of Ministry of Education, School of Chemistry and Chemical Engineering, Shaanxi Normal University, Xi'an, 710062, P. R. China. E-mail: c.wang@snnu.edu.cn*
[b]*Liverpool Centre for Materials and Catalysis, Department of Chemistry, University of Liverpool, Liverpool, L69 7ZD, UK. E-mail: j.xiao@liv.ac.uk; Tel: +44 (0)-1517942937*
[c]*Christopher Ingold Laboratories, Department of Chemistry, University College London, 20 Gordon Street, London, WC1H 0AJ, UK*

†Dedicated to Professor David Cole-Hamilton on the occasion of his retirement and for his outstanding contribution to transition metal catalysis.

‡Electronic supplementary information (ESI) available. CCDC 888574–888577. For ESI and crystallographic data in CIF or other electronic format see DOI: 10.1039/c2dt31368e

MeOH. For example, by simply stirring $[Cp^*IrCl_2]_2$ and ketimines in MeOH at 40 °C for 4 h, the cyclometalated complexes were isolated with similar yields (Scheme 1). Apart from complexes **1** and **2**, which we have used in transfer hydrogenative reductive amination,[8] complex **3**, having an imine ligand derived from an aliphatic amine, was also successfully prepared (Scheme 1).

These complexes have been characterised by NMR and X-ray diffraction. Interestingly, in the $^1$H NMR spectra of complexes **1** and **2**, the *N*-aryl ring displays distinct signals at low temperature and room temperature. For complex **1** at 253 K, the four aromatic protons of its *p*-anisidine part appeared as four well separated, sharp apparent doublet peaks at 7.77, 7.02, 6.94 and 6.83 ppm, all with coupling constant of 8.0 Hz. However, when the $^1$H NMR was measured at 298 K, broad peaks were observed for the four protons of the *p*-anisidine, while the other peaks remained the same as those at 253 K. Particularly, the peaks at 7.02, 6.94 and 6.83 ppm merged into one very broad peak ranging from 7.10 to 6.60 ppm. Similarly, for complex **2** at 253 K, four sharp doublet peaks, with coupling constant of 8.0 Hz, were observed for the four protons from the *p*-anisidine part in the $^1$H NMR. The chemical shifts of these peaks are 7.80, 6.98, 6.90 and 6.81 ppm. Raising the temperature to 298 K, the peaks at 6.98, 6.90 and 6.81 ppm merged into one broad peak ranging from 7.00 to 6.60 ppm. This broadening probably results from the *N*-aryl ring undergoing a rocking motion (*vide infra*). No such NMR pattern was observed for complexes prepared from aldimines, however.[2,3]

As we have reported preciously, complexes **1** and **2** are excellent catalysts for transfer hydrogenation of imines using the HCOOH–$Et_3N$ azeotrope as hydrogen source.[8] The key intermediates during the catalysis are the corresponding iridium hydride complexes generated from formate decarboxylation. Treatment of **1** and **2** with 4 equivalents of HCOOH–$Et_3N$ azeotrope in MeOH resulted in the formation of red and orange crystals, respectively. Analysis of these crystals showed that they are the hydride complexes **4** and **5** (Scheme 2). This is the first time when a cyclometalated Cp*Ir hydride complex has been isolated. The characteristic hydride peaks for **4** and **5** appear at −16.45 and −16.19 ppm, respectively, and as with **1** and **2**, the aromatic protons of their *p*-anisidine substitute are broad in the $^1$H NMR spectra at room temperature.

In preliminary studies, we showed that the hydride reacts readily with iminium salts, but not with neutral imines. Thus, when complex **4** was reacted, in $CD_2Cl_2$ at ambient temperature, with a stoichiometric amount of a benchmark imine prepared from acetophenone and *p*-anisidine, no amine signal was observed in the $^1$H NMR spectra, with the hydride resonance observable even after 8 h. In contrast, **4** reacted with the corresponding iminium tetrafluoroborate salt almost instantly, affording the amine product as shown by $^1$H NMR. These observations are consistent with the involvement of the hydride in the catalytic transfer hydrogenation, with the hydride transfer occurring *via* the ionic-type mechanism.[9,11–14]

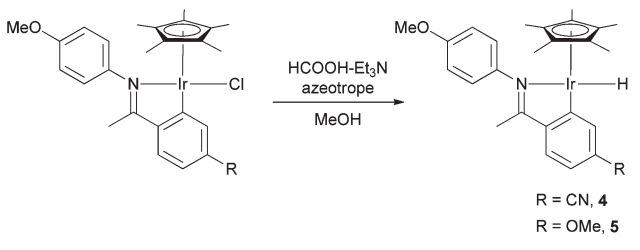


**Scheme 2** Synthesis of cyclometalated iridium hydrides.

## X-ray diffraction structures

Single crystals suitable for X-ray crystallography analysis were grown for compounds **1–5** and their X-ray diffraction structures have been determined. Single crystals of complexes **1–3** were obtained by diffusion of hexane into a $CH_2Cl_2$ solution, whereas those of complexes **4** and **5** formed during their preparation process. Table 1 summarises crystallographic data and parameters, and Fig. 2–6 show the molecular diagram views of complexes **1–5**.[15]

Selected bond distances and angles of complexes **1–3** and **4**, **5** are shown in Tables 2 and 3, respectively. Piano-stool style geometries are observed for all complexes. Compound **1** crystallises in the space group $P\bar{1}$ with 2 independent [Cp*IrClL] molecules in the asymmetric unit. The differences in the bond distances and angles between them are very small, however. Although electronically different, complexes **1–3** display similar Ir–C3, Ir–N, and Ir–Cl bond distances and similar N1–Ir–C3 chelate angles. The Cp* ligand in complexes **1–3** shows a $\eta^3$–$\eta^2$ coordination pattern, with three short Ir–C bond lengths and two longer ones (Table 2). Similar observations were reported by Davies and co-workers.[2] On going from **1** and **2** to **4** and **5**, the changes in the Ir–C3, Ir–N, and Ir–Cl bond distances appear insignificant. However, the Cp* ligand becomes significantly further away from the iridium, presumably reflecting a stronger *trans* effect of the hydride than chloride. Further, the coordination mode of the Cp* somehow changes to $\eta^1$–$\eta^4$, with one of the Ir–C bond distances being significantly shorter (Table 3). In all the complexes, the longest Ir–C bond is that *trans* to the Ir–C3 bond.

The aryl ring substituents on the nitrogen of complexes **1**, **2**, **4** and **5** are almost parallel to the Cp* and sit in between the methyl group of Cp* and that of the ketimine ligand. The closest contact is seen between the methyl group (C9) and the aryl ring of *p*-anisidine, with C···H distances ranging from 2.490 to 2.539 Å, which suggests significant CH–π interactions.[16–18] The sandwich position of the phenyl ring and the CH–π interactions provide an explanation to its $^1$H NMR spectra aforementioned. Space filling model indicates that the aryl ring is not likely to be able to freely rotate along the C–N bond; however, rocking is possible, thereby broadening the resonances of the four chemically different aryl protons in the $^1$H NMR spectra. At low temperature, such rocking may be frozen due partly to the CH–π interactions. As a result, the four protons appear in separated, sharp resonances.

 

**Table 1** Crystallography data of **1–5**

| Compound reference | **1** | **2** | **3** | **4** | **5** |
|---|---|---|---|---|---|
| Chemical formula | $2(C_{26}H_{28}ClIrN_2O)\cdot CH_2Cl_2$ | $C_{26}H_{31}ClIrNO_2$ | $C_{24}H_{33}ClIrN$ | $C_{26}H_{29}IrN_2O$ | $C_{26}H_{32}IrNO_2$ |
| Formula mass | 1309.23 | 617.17 | 563.17 | 577.71 | 582.73 |
| Crystal system | Triclinic | Triclinic | Monoclinic | Monoclinic | Monoclinic |
| $a$/Å | 8.5009(6) | 9.8489(12) | 11.2929(18) | 30.885(10) | 7.1562(7) |
| $b$/Å | 15.6926(12) | 10.6037(13) | 13.525(2) | 9.215(3) | 31.863(3) |
| $c$/Å | 19.8638(13) | 11.3906(14) | 14.951(2) | 16.691(5) | 9.9929(10) |
| $\alpha$/° | 95.170(2) | 90.6560(10) | 90.00 | 90.00 | 90.00 |
| $\beta$/° | 93.4780(10) | 98.1770(10) | 108.771(2) | 98.318(7) | 100.2420(10) |
| $\gamma$/° | 105.6570(10) | 95.502(2) | 90.00 | 90.00 | 90.00 |
| Unit cell volume/Å$^3$ | 2531.2(3) | 1171.7(2) | 2162.1(6) | 4700(3) | 2242.3(4) |
| Temperature/K | 100(2) | 100(2) | 100(2) | 100(2) | 100(2) |
| Space group | $P\bar{1}$ | $P\bar{1}$ | $P21/c$ | $C2/c$ | $P21/n$ |
| No. of formula units per unit cell, $Z$ | 2 | 2 | 4 | 8 | 4 |
| No. of reflections measured | 19 362 | 7159 | 16 589 | 10 502 | 12 832 |
| No. of independent reflections | 11 113 | 5144 | 5344 | 4560 | 4905 |
| $R_{int}$ | 0.0186 | 0.0230 | 0.0279 | 0.0548 | 0.0313 |
| Final $R_1$ values ($I > 2\sigma(I)$) | 0.0230 | 0.0261 | 0.0220 | 0.0650 | 0.0430 |
| Final w$R(F^2)$ values ($I > 2\sigma(I)$) | 0.0496 | 0.0655 | 0.0514 | 0.1597 | 0.0749 |
| Final $R_1$ values (all data) | 0.0283 | 0.0277 | 0.0245 | 0.0813 | 0.0539 |
| Final w$R(F^2)$ values (all data) | 0.0510 | 0.0662 | 0.0522 | 0.1688 | 0.0772 |

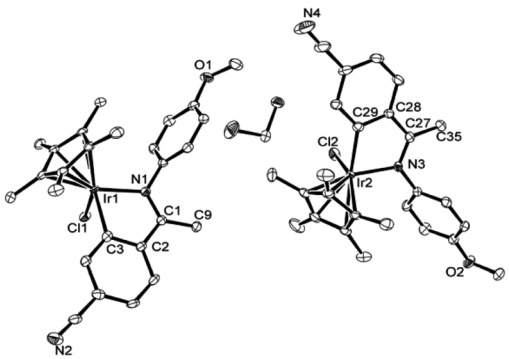


**Fig. 2** Molecular structure of **1**; thermal ellipsoids are drawn at the 50% probability level; hydrogen atoms are omitted for clarity.

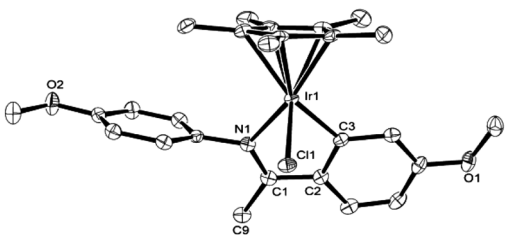


**Fig. 3** Molecular structure of **2**; thermal ellipsoids are drawn at the 50% probability level; hydrogen atoms are omitted for clarity.

## Computer modelling

Complexes **1** and **2** show some difference in transfer hydrogenation. More striking is that the analogous amino complex **6** is almost inactive under the same conditions. To gain insight into this difference, we calculated the frontier molecular orbitals of the hydrides **4**, **5**, and **7** which is expected to form from **6** (Fig. 7).[8,9] The structural properties of complexes **4** and **5** computed at different levels of theory compared with those obtained from experiments are shown in Table S1,‡ which

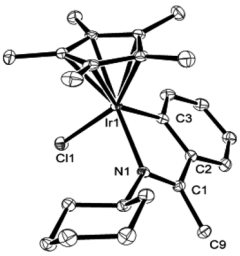


**Fig. 4** Molecular structure of **3**; thermal ellipsoids are drawn at the 50% probability level; hydrogen atoms are omitted for clarity.

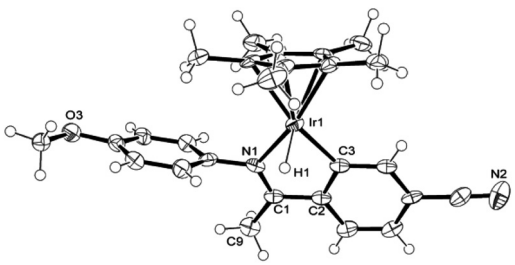


**Fig. 5** Molecular structure of **4**; thermal ellipsoids are drawn at the 50% probability level.

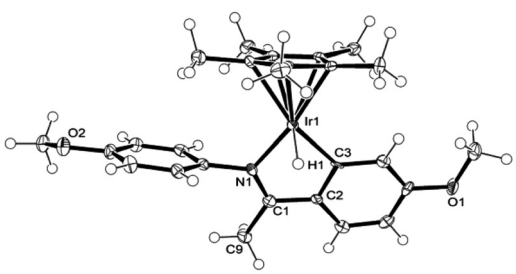


**Fig. 6** Molecular structure of **5**; thermal ellipsoids are drawn at the 50% probability level.

**Table 2** Select bond distances (Å) and angles (°) of **1–3**

| | 1 | 2 | 3 |
|---|---|---|---|
| Ir(1)–Cl(1) | 2.400(8) | 2.405(10) | 2.399(7) |
| Ir(1)–C(3) | 2.024(3) | 2.028(3) | 2.016(3) |
| Ir(1)–N(1) | 2.085(3) | 2.094(3) | 2.114(2) |
| C(1)–C(2) | 1.460(4) | 1.454(5) | 1.457(3) |
| C(1)–C(9) | 1.490(4) | 1.505(5) | 1.501(4) |
| C(1)–N(1) | 1.308(4) | 1.286(5) | 1.303(3) |
| C(2)–C(3) | 1.414(4) | 1.417(5) | 1.417(4) |
| Ir(1)–C(Cp*) | 2.156(3) | 2.138(4) | 2.153(3) |
| | 2.158(3) | 2.154(4) | 2.155(3) |
| | 2.158(3) | 2.167(3) | 2.159(3) |
| | 2.265(3) | 2.248(3) | 2.288(3) |
| | 2.284(3) | 2.272(4) | 2.320(3) |
| C(1)–N(1)–Ir(1) | 118.7(2) | 118.2(2) | 116.48(18) |
| C(1)–C(2)–C(3) | 114.6(3) | 113.9(3) | |
| C(2)–C(1)–N(1) | 113.2(3) | 114.5(3) | 115.1(2) |
| C(2)–C(3)–Ir(1) | 115.8(2) | 115.6(2) | |
| C(3)–Ir(1)–N(1) | 77.28(11) | 76.95(13) | 77.56(9) |
| C(3)–Ir(1)–Cl(1) | 86.12(10) | 87.81(11) | 88.71(8) |
| Cl(1)–Ir(1)–N(1) | 87.39(7) | 85.14(9) | 89.34(6) |
| C(9)–C(1)–N(1) | 124.4(3) | 123.4(3) | 123.8(2) |
| C(9)–C(1)–C(2) | 122.4(3) | 122.2(3) | 121.1(2) |

**Table 3** Select bond distances (Å) and angles (°) of **4** and **5**

| | 4 | 5 |
|---|---|---|
| Ir(1)–H(1) | 1.740 | 1.714 |
| Ir(1)–C(3) | 2.043(10) | 2.048(5) |
| Ir(1)–N(1) | 2.088(9) | 2.033(5) |
| C(1)–C(2) | 1.465(14) | 1.441(8) |
| C(1)–C(9) | 1.511(17) | 1.491(8) |
| C(1)–N(1) | 1.307(15) | 1.324(8) |
| C(2)–C(3) | 1.430(13) | 1.406(8) |
| Ir(1)–C(Cp*) | 2.211(12) | 2.167(6) |
| | 2.262(10) | 2.231(6) |
| | 2.264(10) | 2.251(5) |
| | 2.270(12) | 2.259(6) |
| | 2.292(10) | 2.266(6) |
| C(1)–N(1)–Ir(1) | 120.1(7) | 119.9(4) |
| C(1)–C(2)–C(3) | 114.0(9) | 115.9(5) |
| C(2)–C(1)–N(1) | 113.1(10) | 112.4(5) |
| C(2)–C(3)–Ir(1) | 116.2(7) | 114.1(4) |
| C(3)–Ir(1)–N(1) | 76.6(4) | 77.7(2) |
| C(3)–Ir(1)–H(1) | 87.00 | 86.4 |
| H(1)–Ir(1)–N(1) | 81.00 | 88.8 |
| C(9)–C(1)–N(1) | 124.6(9) | 125.2(6) |
| C(9)–C(1)–C(2) | 122.4(9) | 122.3(6) |

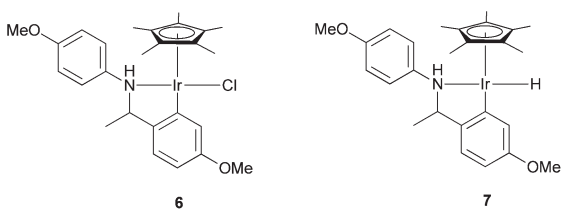


**Fig. 7** Complex **6** and the hydride **7** derived thereof.

reveals that the modelled structures fit well with experimental results. The hydride 7 exists in two configurations, *cis*-7 in which the NH proton is *cis* positioned to the hydride ligand and *trans*-7 where the NH proton and hydride are *trans* to each other, shown in Fig. S1.‡ The *cis*-7 is 1.36 kcal mol$^{-1}$ more stable than *trans*-7. The computed structural properties of the two hydrides are given in Table S1.‡

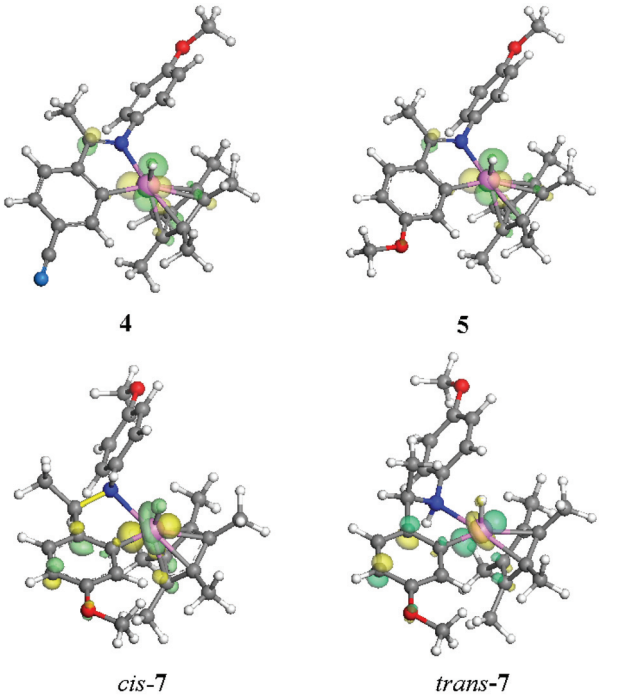


**Fig. 8** HOMO orbitals for **4**, **5**, *cis*-**7** and *trans*-**7**. Top left: HOMO of **4**; top right: HOMO of **5**; bottom left: HOMO of *cis*-**7**; bottom right: HOMO of *trans*-**7**.

**Table 4** HOMO–LUMO energies (eV) of **4**, **5**, **7** and substrate

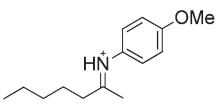


| | 4 | 5 | *cis*-7 | |
|---|---|---|---|---|
| Charge of H(–Ir) | −0.063 | −0.068 | −0.087 | −0.55(N=C) |
| Charge of Ir(–H) | 0.111 | 0.104 | 0.083 | 0.38(C=N) |
| HOMO | −5.31 | −4.93 | −4.85 | −9.80 |
| LUMO | −1.58 | −0.72 | −0.27 | −5.71 |

The frontier orbitals (HOMO) of the three hydrides are shown in Fig. 8. We note that the orbital shapes of **4** and **5** are similar but are different from *cis*-7 and *trans*-7. Further, the electrons are situated mainly in the $d_{yz}$ orbital of **4** and **5** where an imine bonds to iridium but mainly in the $d_{z^2}$ of 7 with an amine bonded to iridium. This may affect how the Ir–H hydride interacts with an incoming iminium C=N bond in the hydride transfer step. Turning to the energy levels of HOMO and LUMO of compound **4**, **5** and *cis*-7 shown in Table 4, we note that the HOMO of **4** is closest to, and that of *cis*-7 is furthest away from, the LUMO of the substrate, an iminium cation. If the transfer hydrogenation aforementioned is limited by the step of hydride transfer in the turnover rate,

this HOMO–LUMO separation is expected to impact on the hydrogenation rate; the smaller the gap the faster the rate would be. We also calculated the charge on the hydride and iridium (Table 4); however the difference between **4**, **5** and *cis*-**7** appears to be insignificant.

## Conclusions

In this paper, the synthesis and X-ray diffraction structures of five cyclometalated iridium complexes are described. The two hydrides are the first examples of isolated and structurally characterised cyclometalated iridium hydride complexes, which have been suggested to be involved in a number of hydrogenation reactions.[9,18] Computational studies were carried out, revealing difference in the frontier orbitals of active and inactive hydrides.

## Experimental

Unless otherwise specified, the chemicals were obtained commercially and used without further purification. Experiments were carried out using standard Schlenk technique. Dichloromethane was dried over $CaH_2$ and distilled prior to use. MeOH were dried over magnesium and distilled prior to use. NMR spectra were recorded on a Bruker 400 Hz NMR spectrometer with TMS as the internal standard. NMRs for complex **1** and **2** were carried out at 253 K. NMRs for **3–5** were carried out at 298 K. Imine ligands were prepared according to the literature.[19]

### General procedure for preparation of 1–3

$[Cp^*IrCl_2]_2$ (1 equiv.), an imine ligand (2.2 equiv.) and NaOAc (10 equiv.) were placed into a Schlenk tube. The tube was then degassed and recharged with nitrogen three times. $CH_2Cl_2$ was then added and the resulting mixture was stirred at room temperature overnight. The reaction mixture was filtered through celite, and dried over $MgSO_4$. Following removal of the solvent under vacuum the resulting solid was washed with diethyl ether/hexane to afford pure compounds. Complex **3** was purified by flash chromatography on silica gel using hexane/ethyl acetate solvent system as eluent. Single crystals suitable for X-ray analysis were obtained by diffusion of hexane into a $CH_2Cl_2$ solution.

**1**. 88% yield as a red solid, melting point 227–229 °C; $^1$H NMR ($CDCl_3$, 400 MHz, 253 K) $\delta$ (ppm): 8.05 (d, $J$ = 1.4 Hz, 1H), 7.76 (d, $J$ = 8.6 Hz, 1H), 7.56 (d, $J$ = 7.8 Hz, 1H), 7.33 (dd, $J$ = 8.0 Hz, 1.5 Hz, 1H), 7.01 (d, $J$ = 8.7 Hz, 1H), 6.95–6.93 (m, 1H), 6.84–6.79 (m, 1H), 3.88 (s, 3H), 2.48 (s, 3H), 1.44 (s, 15H); $^{13}$C NMR ($CDCl_3$, 100 MHz, 253 K) $\delta$ (ppm): 180.9, 167.4, 157.9, 151.8, 143.6, 138.3, 138.2, 128.2, 125.2, 123.1, 120.1, 115.1, 114.3, 112.5, 90.0, 55.7, 17.5, 8.8; HRMS (ESI) for $C_{25}H_{29}ClIrNO$ $[M + NH_4]^+$: calc.: 628.2834. Found: 628.2826. $[M - Cl]^+$: calc.: 575.1802. Found: 575.1799.

**2**. 90% yield as a yellow solid, melting point 205–206 °C; $^1$H NMR ($CDCl_3$, 400 MHz, 253 K) $\delta$ (ppm): 7.79 (d, $J$ = 7.9 Hz, 1H), 7.48 (d, $J$ = 8.5 Hz, 1H), 7.35 (d, $J$ = 2.5 Hz, 1H), 6.98 (d, $J$ = 8.6 Hz, 1H), 6.89 (d, $J$ = 8.5 Hz, 1H), 6.81 (d, $J$ = 7.8 Hz, 1H), 6.60 (dd, $J$ = 8.5, 2.5 Hz, 1H), 3.93 (s, 3H), 3.87 (s, 3H), 2.41 (s, 3H), 1.44 (s, 15H); $^{13}$C NMR ($CDCl_3$, 100 MHz, 253 K) $\delta$ (ppm): 180.0, 170.1, 161.7, 157.1, 144.0, 141.0, 130.0, 125.0, 123.6, 118.9, 114.7, 112.0, 107.5, 88.8, 55.4, 55.0, 16.9, 8.6; Anal. calc. for $C_{26}H_{31}ClIrNO_2$ (%): C, 50.60, H, 5.06, N, 2.27. Found: C, 50.46, H, 5.03, N, 2.85; HRMS (ESI) for $C_{26}H_{31}ClIrNO_2$ $[M - Cl]^+$: calc.: 580.1955. Found: 580.1952. HRMS (EI) for $C_{26}H_{31}ClIrNO_2$ $[M]^+$: calc.: 615.1644. Found: 615.1646.

**3**. 60% yield as a yellow solid; $^1$H NMR ($CD_2Cl_2$, 400 MHz, 298 K) $\delta$ (ppm): 7.72 (dd, $J$ = 7.6, 0.9 Hz, 1H), 7.39 (dd, $J$ = 7.8, 1.2 Hz, 1H), 7.13 (dt, $J$ = 7.4, 1.4 Hz, 1H), 6.96–6.92 (m, 1H), 4.21–4.13 (m, 1H), 2.68 (s, 3H), 2.21–2.18 (m, 2H), 2.04–1.70 (m, 20H), 1.48–1.23 (m, 3H); $^{13}$C NMR ($CDCl_3$, 100 MHz, 298 K) $\delta$ (ppm): 179.2, 167.0, 149.2, 134.9, 131.2, 127.1, 121.1, 89.0, 70.2, 32.6, 31.1, 26.0, 25.5, 25.4, 17.8, 9.7; Anal. calc. for $C_{24}H_{33}ClIrN$ (%): C, 51.18, H, 5.91, N, 2.49. Found: C, 51.50, H, 6.09, N, 2.40.

### Typical procedure for preparation of 2 in MeOH

$[Cp^*IrCl_2]_2$ (1 equiv.), an imine ligand (2.2 equiv.) were placed into a Schlenk tube. The tube was then degassed and recharged with nitrogen three times. MeOH was then added and the resulting mixture was stirred at 40 °C for 4 h. MeOH was removed and the resulting solid was re-dissolved in $CH_2Cl_2$. The solution was then washed with aqueous $NaHCO_3$ solution and water. The organic layer was dried over $MgSO_4$. After filtration and removal of $CH_2Cl_2$ under vacuum the resulting solid was washed with diethyl ether/hexane to afford pure **2**.

### Typical procedure for preparation of cyclometalated iridium hydrides

Complex **1** (1 equiv.) was placed in a Schlenk tube and degassed. MeOH and FT (4 equiv.) were then introduced. The solution was left overnight; red crystals of **4** were collected after removing the liquid with syringe and washed with MeOH. Complex **5** was prepared following the same procedure.

**4**. 45% yield as red crystals; $^1$H NMR ($CD_2Cl_2$, 400 MHz, 298 K) $\delta$ (ppm): 8.12 (d, $J$ = 1.3 Hz 1H), 7.55 (d, $J$ = 8.1 Hz, 1H), 7.22 (dd, $J$ = 8.1 Hz, 1.6 Hz, 1H), 7.17 (br, 1H), 7.00 (br, 2H), 6.84 (br, 1H), 3.89 (s, 3H), 2.34 (d, $J$ = 1.4 Hz, 3H), 1.70 (s, 15H), −16.45 (s, 1H); $^{13}$C NMR ($CDCl_3$, 100 MHz, 298 K) $\delta$ (ppm): 181.0, 175.1, 168.7, 157.6, 150.0, 145.5, 139.2, 127.9, 121.4, 120.2, 111.2, 90.9, 55.5, 45.9, 16.0, 9.2; Anal. calc. for $C_{26}H_{29}IrN_2O$ (%): C, 54.05, H, 5.06, N, 4.85. Found: C, 53.63, H, 5.00, N, 4.84.

**5**. 50% yield as orange crystals; $^1$H NMR ($CD_2Cl_2$, 400 MHz, 298 K) $\delta$ (ppm): 7.30 (d, $J$ = 8.6 Hz, 1H), 7.22 (d, $J$ = 2.5 Hz, 1H), 7.05 (br, 1H), 6.88 (br, 2H), 6.72 (br, 1H), 6.44 (dd, $J$ = 8.6, 2.6 Hz, 1H), 3.81 (s, 3H), 3.76 (s, 3H), 2.16 (d, $J$ = 1.3 Hz, 3H), 1.58 (s, 15H), −16.19 (s, 1H); $^{13}$C NMR ($CDCl_3$, 100 MHz, 298 K) $\delta$ (ppm): 179.2, 173.0, 169.8, 158.8, 155.4, 144.2, 138.7,

127.9, 125.1, 116.3, 104.6, 88.1, 53.8, 53.2, 14.1, 7.7; Anal. calc. for $C_{26}H_{32}IrNO_2$ (%): C, 53.59, H, 5.53, N, 2.40. Found: C, 53.09, H, 5.38, N, 2.24.

### Computational details

Density functional theory (DFT) calculations were carried out using the DMol$^3$ code, where the wave function is expanded in a localised atom-centred basis set with each basis function defined numerically, on a dense radial grid. In this study, we employed the double-numeric-polarised (DNP) basis set. Each basis function was restricted to within a cutoff radius of 4.7 Å. The electron density was approximated using a multipolar expansion up to octupole. For total energies and geometry optimisation, the gradient corrected PBE exchange-correlation functional was employed. The inner core-electrons for iridium were represented by the Density functional Semi-core Pseudo Potentials (DSPP), which was generated by fitting all-electron relativistic DFT results, and specifically developed to improve the accuracy of DMol$^3$ calculations. In the optimisation procedure, the geometry was considered to be converged when the energy change was less than $10^{-5}$ Hartree and the gradient was less than $2 \times 10^{-3}$ Hartree Å$^{-1}$. In Gaussian 03, the PBE0, B3LYP and MPW1PW91 hybrid exchange-correlation functionals were employed. We also compared different basis sets — 6-31G(d,p), 6-311G(d,p), 6-31+G(d,p), 6-311+G(d,p), 6-31++G(d,p) and 6-311++G(d,p) — for hydrogen, carbon, nitrogen and oxygen; for iridium, we used the SDD and LANL2DZ basis set coupled with the SDD and LANL2 pseudopotentials respectively.

Different exchange correlation functionals and basis sets have been examined using DMol$^3$ and Gaussian 03, compared with the experimental bond lengths and bond angles of complexes **4** and **5**, shown in Table S1 (ESI‡). The HOMO and LUMO orbitals and their energy values are obtained using Gaussian 03. The charges are obtained using ESP charge using DMol$^3$.

## Acknowledgements

We are grateful to Pfizer for funding (C.W.) and AstraZeneca for support.

## Notes and references

1 M. Albrecht, *Chem. Rev.*, 2009, **110**, 576–623.
2 D. L. Davies, O. Al-Duaij, J. Fawcett, M. Giardiello, S. T. Hilton and D. R. Russell, *Dalton Trans.*, 2003, 4132–4138.
3 L. Li, W. W. Brennessel and W. D. Jones, *Organometallics*, 2009, **28**, 3492–3500.
4 S. Arita, T. Koike, Y. Kayaki and T. Ikariya, *Organometallics*, 2008, **27**, 2795–2802.
5 T. Jerphagnon, A. J. A. Gayet, F. Berthiol, V. Ritleng, N. Mršić, A. Meetsma, M. Pfeffer, A. J. Minnaard, B. L. Feringa and J. G. de Vries, *Chem.–Eur. J.*, 2009, **15**, 12780–12790.
6 J. F. Hull, D. Balcells, J. D. Blakemore, C. D. Incarvito, O. Eisenstein, G. W. Brudvig and R. H. Crabtree, *J. Am. Chem. Soc.*, 2009, **131**, 8730–8731.
7 Y. Kashiwame, S. Kuwata and T. Ikariya, *Chem.–Eur. J.*, 2010, **16**, 766–770.
8 C. Wang, A. Pettman, J. Bacsa and J. Xiao, *Angew. Chem., Int. Ed.*, 2010, **49**, 7548–7552.
9 C. Wang, B. Villa-Marcos and J. Xiao, *Chem. Commun.*, 2011, **47**, 9773–9785.
10 D. L. Davies, S. M. A. Donald, O. Al-Duaij, S. A. Macgregor and M. Pölleth, *J. Am. Chem. Soc.*, 2006, **128**, 4210–4211.
11 S. E. Clapham, A. Hadzovic and R. H. Morris, *Coord. Chem. Rev.*, 2004, **248**, 2201–2237.
12 R. M. Bullock, *Chem.–Eur. J.*, 2004, **10**, 2366–2374.
13 J. B. Aberg, J. S. M. Samec and J.-E. Bäckvall, *Chem. Commun.*, 2006, 2771–2773.
14 H. F. Zhou, Z. W. Li, Z. J. Wang, T. L. Wang, L. J. Xu, Y. He, Q. H. Fan, J. Pan, L. Q. Gu and A. S. C. Chan, *Angew. Chem., Int. Ed.*, 2008, **47**, 8464–8467.
15 The structure of **1** was given in the supporting information of ref. 8. For comparison, it is described here.
16 M. Nishio, M. Hirota and Y. Umezawa, in *The CH/π Interaction: Evidence, Nature, and Consequences*, ed. A. P. Marchand, Wiley-VCH, New York, 1998.
17 S. V. Lindeman, D. Kosynkin and J. K. Kochi, *J. Am. Chem. Soc.*, 1998, **120**, 13268–13269.
18 R. Noyori, M. Yamakawa and S. Hashiguchi, *J. Org. Chem.*, 2001, **66**, 7931–7944.
19 J. S. M. Samec and J.-E. Bäckvall, *Chem.–Eur. J.*, 2002, **8**, 2955–2961.

 